Orally Bioavailable Peptides

DOI: 10.1002/anie.201405364

Improving on Nature: Making a Cyclic Heptapeptide Orally Bioavailable**

*Daniel S. Nielsen, Huy N. Hoang, Rink-Jan Lohman, Timothy A. Hill, Andrew J. Lucke, David J. Craik, David J. Edmonds, David A. Griffith, Charles J. Rotter, Roger B. Ruggeri, David A. Price, Spiros Liras, and David P. Fairlie**

Abstract: *The use of peptides in medicine is limited by low membrane permeability, metabolic instability, high clearance, and negligible oral bioavailability. The prediction of oral bioavailability of drugs relies on physicochemical properties that favor passive permeability and oxidative metabolic stability, but these may not be useful for peptides. Here we investigate effects of heterocyclic constraints, intramolecular hydrogen bonds, and side chains on the oral bioavailability of cyclic heptapeptides. NMR-derived structures, amide H–D exchange rates, and temperature-dependent chemical shifts showed that the combination of rigidification, stronger hydrogen bonds, and solvent shielding by branched side chains enhances the oral bioavailability of cyclic heptapeptides in rats without the need for N-methylation.*

Peptides are a rich natural source of chemical diversity that is underexploited in medicine, principally because they are metabolically unstable and too polar for intestinal absorption or plasma retention after oral ingestion.[1] Cyclization makes peptides more stable to proteolytic enzymes, such as aminopeptidases and carboxypeptidases, that cleave off amino acids from their N- and C-termini, respectively, and digestive proteases in the gastrointestinal tract that recognize and hydrolyze extended strand-like peptide conformations.[2] Nature modifies cyclic peptides for enhanced membrane permeability by reducing hydrogen-bond donors (e.g., by replacing NH with *N*-methyl, N-heterocycle, and O) and by minimizing water solvation of amides (e.g., by forming transannular hydrogen bonds and by shielding polar atoms using hydrophobic side chains). These are reasons for the atypical oral bioavailability of the natural product drug cyclosporin A,[3] an 11-residue cyclic peptide, which is flexible and exists in multiple conformations.[4] This flexibility reportedly inspired the discovery of an orally bioavailable synthetic cyclic hexapeptide.[5a] However, there have been surprisingly few reports of cyclic peptides that have been rationally modified to enhance both membrane permeability[6] and oral bioavailability.[5] Here we set out to use three-dimensional solution structural information to design changes to a marine natural product, the cyclic heptapeptide sanguinamide A,[7] to increase intestinal permeability and oral bioavailability. This approach may be valuable in understanding key principles for rationally designing orally bioavailable peptides.

Simple head-to-tail cyclization of Ile–Ala–Ala–Phe–Pro–Ile–Pro to a cyclic heptapeptide (**1**, Figure 1) was first examined to understand how further constraints can influence the structure and oral absorption of sanguinamide A (**2**, Figure 2) and analogues. NMR spectra for **1** showed the presence of two conformers (**1a**, **1b**) arising from *cis–trans* isomerization at Ile5–Pro6 and a *cis*-amide at Phe3–Pro4. This equilibrium is not uncommon for cyclic peptides containing proline and/or *N*-methyl amino acids. Unlike cyclosporin A, which adopts interconverting conformations in

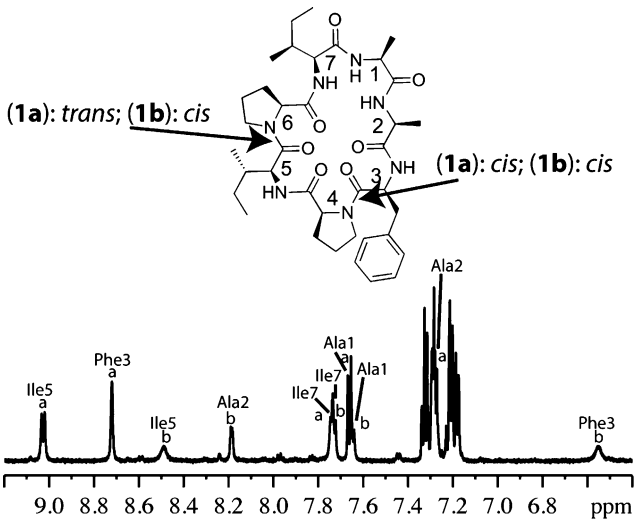

Figure 1. Cyclo-[Ile–Ala–Ala–Phe–Pro–Ile–Pro] (**1**) and its 600 MHz ^{1}H NMR spectrum (amide region) in [D$_6$]DMSO. Two sets of amide protons are due to *cis*-3/4, *trans*-5/6 (**1a**), and *cis*-3/4, *cis*-5/6 (**1b**) isomers (ratio 2:1).

[*] D. S. Nielsen, Dr. H. N. Hoang, Dr. R. J. Lohman, Dr. T. A. Hill, Dr. A. J. Lucke, Prof. Dr. D. J. Craik, Prof. Dr. D. P. Fairlie
Division of Chemistry and Structural Biology, University of Qld
Brisbane, Qld 4072 (Australia)
E-mail: d.fairlie@imb.uq.edu.au
Dr. D. J. Edmonds, Dr. D. A. Griffith, Dr. R. B. Ruggeri, Dr. D. A. Price, Dr. S. Liras
World Wide Medicinal Chemistry, CVMED, Pfizer
Cambridge, MA (USA)
C. J. Rotter
Pfizer Pharmacokinetics, Dynamics and Metabolism
Groton, CT (USA)

[**] We thank Gilles Goetz for EPSA measurements; the Australian Research Council (LP110200213, F0668733, DP1096290, CE140100011), and the Queensland Government (CIF) for funding, and the Australian National Health and Medical Research Council for Senior Principal Research Fellowships to D.C. (1026501) and D.F. (1027369).

Supporting information for this article is available on the WWW under http://dx.doi.org/10.1002/anie.201405364.

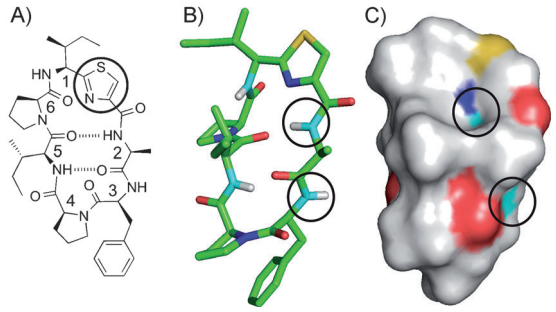

Figure 2. Sanguinamide A (**2**) showing A) molecular structure with thiazole circled, B) NMR-derived solution structure ([D_6]DMSO), and C) solvent-exposed surface, with hydrogen bonds (dashed lines), amide NH nitrogen atoms (cyan), and two exposed amide NH protons (circles).

Table 1: H–D exchange rates (90% [D_6]DMSO, 10% D_2O) and NMR temperature coefficients ([D_6]DMSO) for amide NH protons of **2**–**4**.

Cyclic Peptide	**2**[a]	**3**	**4**
Amide NH H–D exchange $t_{1/2}$ (min, 298 K)			
Ile1 (Thz)	1500	1400	2000
Ala2 or *t*BuGly2	188	5600	21 000
Phe3	380	–	387
Ile5	6000	5500	15 000
Amide NH temperature coefficient $\Delta\delta/T$ [ppb/K]			
Ile1 (Thz)	−4.0	−2.9	−2.9
Ala2 or *t*BuGly2	−2.9	−0.3	0.005
Phe3	−4.2	–	−3.9
Ile5	−4.0	−1.6	−1.8

[a] See Ref. [7] for additional NMR data.

solution, *cis–trans* isomers of **1** have high energetic barriers to interconversion.

We have previously reported the total synthesis of sanguinamide A, cyclo-[Ile(Thz)–Ala–Phe–Pro–Ile–Pro] (**2**, Figure 2), a thiazole-containing cyclic peptide analogue of **1** isolated from the sea slug *H. sanguineus*.[7] It features all L-amino acids, phenylalanine, alanine, isoleucine, two prolines, and an isoleucine-thiazole dipeptide surrogate. The latter heterocycle helps to rigidify the cyclic peptide **2**, which adopts a single conformation with only one *cis*-amide (Phe3–Pro4). This conformation has two strong intramolecular hydrogen bonds between Ala2 and Leu5 (Figure 2). It has molecular properties that are both expected [hydrogen bond donors (HBD) = 4, rotatable bonds (RotB) = 6] and not expected [MW = 721, hydrogen bond acceptors (HBA) = 13, calculated partition coefficient (CLogP) = 5.5, topological polar surface area (tPSA) = 169 Å^2][8] to favor oral bioavailability, yet compound **2** exhibited some bioavailability after oral delivery at 10 mg kg^{-1} to male Wistar rats (F = 7%, C_{max} 40 nM, T_{max} 60 min), despite rapid clearance (70 mL min^{-1} kg^{-1}) and a short half-life ($t_{1/2}$ 23 min).[7] The oral availability of **2** is attributed to 1) three heterocycles replacing three amide NH protons in a heptapeptide, reducing HBD by three; 2) shielding of several polar atoms from water by hydrophobic side chains (Ile1, Pro4, Ile5, Pro6); and 3) two intramolecular hydrogen bonds (Ala2 NH···OC Ile5, Ala2 CO···HN Ile5) that force polar atoms to the interior of the macrocycle. We now propose further changes designed to decrease solvent exposure of its polar surface in order to increase membrane permeability and oral bioavailability.

Of the four amide NH protons in **2**, only two are solvent-exposed (Ala2, Phe3) and visible on the surface shown above (cyan, Figure 2) of the NMR-derived solution structure of **2** in [D_6]DMSO. We set out to N-methylate the more exposed Phe3 NH, thereby reducing the H-bond donor count in **2** to three. Despite the Ala2 NH of **2** being hydrogen-bonded, according to a characteristically low temperature-dependent chemical shift ($\Delta\delta/T = -2.9$ ppb/deg)[9a] and three-dimensional structure analysis indicating that it projects into the interior of the macrocycle to form a H-bond with the Ile5 CO,[7] we find that H–D exchange of Ala2 is still relatively fast (Table 1) consistent with some degree of solvent exposure. We therefore sought to shield this amide bond. We hypothesized that changing Ala2 to the bulkier residue *t*BuGly2 (*tert*-butyl glycine) with a branched hydrophobic side chain might block the solvation of the amide NH at position 2. Together, the two changes, Ala2 to *t*BuGly and Phe3 to *N*-Me-Phe3 resulted in a new cyclic peptide, danamide D (**3**, Figure 3), which was readily synthesized by solid phase synthesis (see the Supporting Information) following the total synthesis of sanguinamide A.[7]

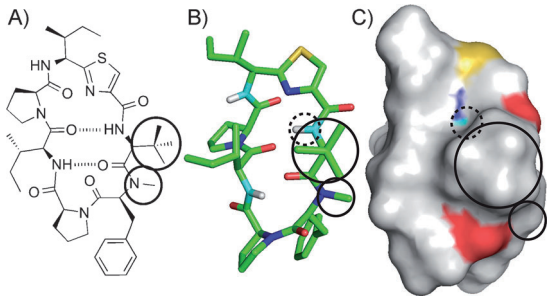

Figure 3. Danamide D (**3**) showing A) molecular structure, B) NMR-derived solution structure ([D_6]DMSO), and C) solvent-exposed surface. Hydrogen bonds (dashed lines), amide NH nitrogen atoms (cyan), changes are in black circles, dashed circle indicates the masked NH.

To test this strategy, 1D ^{1}H NMR experiments were conducted to compare the H–D amide exchange rates and the temperature-dependent amide NH chemical shifts for residues in **2** versus **3** (Table 1). Replacing Ala2 in **2** with the bulkier *tert*-butyl glycine resulted in a slower H–D exchange and a very small temperature effect on the chemical shift of this amide NH (Table 1). These data strongly suggest minimal solvent exposure of this amide NH, which we ascribe to an efficient masking by the *tert*-butyl side chain in **3**. For **2** and **3**, Ile5 NH had a very slow H–D exchange rate and the NMR temperature coefficient for this amide NH decreased to −1.6 ppb/K, indicating that the Ala2 CO···HN Ile5 intramolecular hydrogen bond had not been disrupted. Shielding of the Ile1(Thz) NH was likewise maintained, with little change in H–D exchange rate and only a small change in the NMR temperature coefficient.

The solution structure was determined for **3** in [D_6]DMSO at 298 K using NOESY 2D ^{1}H NMR spectra, calculated from 41 NOE distance restraints, two backbone ϕ-dihedral angle restraints derived from $^3J_{NH\text{-}CH\alpha}$, one *cis*-amide between Phe3–Pro4, and without any hydrogen bond restraints. Structures were calculated in XPLOR-NIH[9b] using a dynamic simulated annealing protocol in a geometric force field and energy-minimized using the CHARMm force field.[9c] The 20 lowest-energy structures (Figure 3B, Figure 5A) for **3** had no distance ($\geq$0.2 Å) or dihedral angle ($\geq$2°) violations and were quite rigid, convergent structures (average pairwise backbone root-mean-square deviation (RMSD) 0.180 Å). The structure of **3** supported the observations made from variable temperature (VT) NMR and H–D exchange experiments (Table 1), with reciprocal *t*BuGly2 CO···HN Ile5 and *t*BuGly2 NH···OC Ile5 hydrogen bonds forming an antiparallel β-sheet connected by a hairpin turn centered at Phe3–Pro4 (Figure 3A). Pro6 and Ile1(Thz) form an α-turn[10] at the other end of **3**. Side chains from Pro4–Ile5–Pro6–Ile1 create a contiguous hydrophobic surface along one side of the molecule (Figure 3C), which shields polar atoms in Ile1 and Ile5 from solvent. Incorporating the bulky *tert*-butyl substituent almost, but not completely, masks the amide proton and carbonyl oxygen of *t*BuGly2 and slightly masks the carbonyl oxygen of Phe3, making these polar atoms less accessible to solvent. The Phe3 NH of **2** was removed by N-methylation, reducing the barrier to rotation around *t*BuGly2–Phe3 to produce two conformations (Figure 5A and B). The common Pro4–Ile5–Pro6 motif in **2** and **3** is also present in other natural products (e.g., dichotomin G,[11a] phakellistatin 1,[11b] 6,[11c] 10,[11d] 17,[11e] 18,[11e] stylopeptide 1,[11f] and stylisin 2[11g]) and may be one way how nature shields the amide backbone to create a contiguous hydrophobic patch (Figure 2, Figure 3) that may be important in peptides for membrane permeability (see below).

The exposed polar surface has therefore been minimized in progressing from **2** to **3** by removing and shielding solvent accessible amide NHs. However, these modifications did not affect the intramolecular hydrogen bonds, with the exception of residue 2 where shielding dampened the H–D exchange. The amide NH of Ile5 suffered a slight but noticeable increase in H–D exchange rate in changing from structure **2** to **3**. We wondered whether amide N-methylation at Phe3, while reducing the number of hydrogen bond donors, might have disrupted the structure by slightly shifting the *tert*-butyl substituent and weakening the hydrogen bond. Although H–D exchange rates and NMR temperature coefficients (Table 1) did not indicate any pronounced increase in flexibility, NMR-structure calculations did suggest more flexibility at the Phe3 residue in **3** versus **2**, after the *N*-methyl group had been introduced. This encouraged us to investigate the structure of the non-N-methylated analogue of **3**, namely **4** (Figure 4).

The solution structure was determined for **4** in [D_6]DMSO at 298 K using NOESY 2D ^{1}H NMR spectra, calculated from 34 NOE distance restraints, four backbone ϕ-dihedral angle restraints derived from $^3J_{NH\text{-}CH\alpha}$, one *cis*-amide between Phe3–Pro4, and without any hydrogen bond restraints. The 20 lowest-energy structures (Figure 4B and Figure 5A) for **4** had no distance ($\geq$0.2 Å) or dihedral angle ($\geq$2°) violations and were rigid, convergent structures (average pairwise backbone RMSD 0.041 Å). The structure of **4** was subtly different from **3**, the *t*Bu substituent now completely masking the amide protons of *t*BuGly2 and Ile5 (Figure 4C), making them less accessible to solvent. Structural differences between **3** and **4** were visualized in more detail by superimposing the

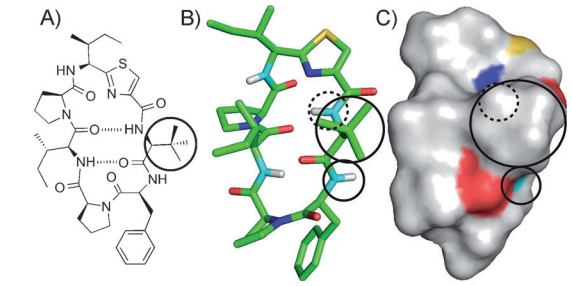

Figure 4. Danamide F (**4**) showing: A) molecular structure, B) NMR-derived solution structure ([D_6]DMSO), and C) solvent-exposed surface. Dashed lines are hydrogen bonds, amide NH nitrogen atoms in cyan, solid circles indicate changes, dashed circles reflect the masked NH.

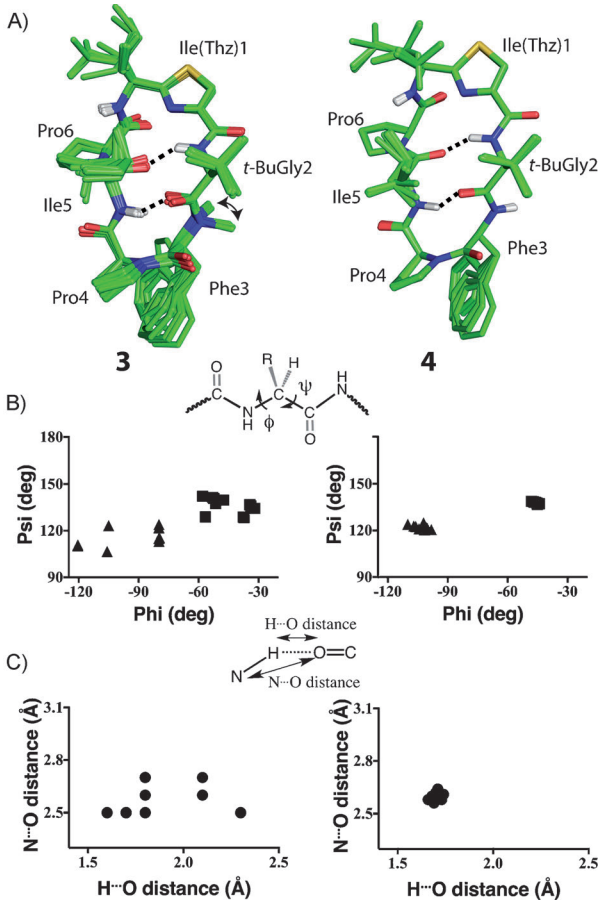

Figure 5. A) Superimposition of 20 lowest-energy solution structures of **3** and **4** with backbone atom pairwise RMSD of 0.18 Å and 0.04 Å, respectively, double arrow line indicates flexibility at Phe3 N-methylated amide; B) phi and psi dihedral angles for Phe3 (square) and Ile5 (triangle) for **3** (left) versus **4** (right); C) the H-bond N···O and N···H lengths for Ile5 NH···OC *t*BuGly2 in **3** (left) versus **4** (right).

20 lowest-energy NMR-solution structures of each compound (Figure 5). Backbone RMSD indicated less conformational flexibility about the Phe3–Pro4 bond and the Ile5–Pro6–Ile1(Thz)–*t*BuGly2 segment in **4** than in **3** (Figure 5A), suggesting a more rigid backbone structure in **4** than in **3**. The higher flexibility in **3** resulted in weaker intramolecular hydrogen bonds between *t*BuGly2 and Ile5 in the 20 lowest-energy structures, measured as changes in phi and psi angles at Phe3 and Ile5 (Figure 5B) and distances between hydrogen bonding atoms (Figure 5C). Although the phi and psi angles were quite different among the 20 lowest-energy structures of **3** (Figure 5B, left), they did not change much and were more clustered in the 20 lowest-energy structures of **4** (Figure 5B, right). Likewise, the H-bond N···O and H···O lengths for Ile5 NH···OC *t*BuGly2 were quite varied for **3** (Figure 5C, left) but did not change across the 20 structures of **4** (Figure 5C, right). These findings were in agreement with surface comparisons of amides in **3** versus **4** (Figure 3 versus Figure 4).

This evidence for decreased flexibility in the peptide backbone, on changing from **3** (RMSD 0.18 Å) with *N*-Me-Phe3 to **4** (RMSD 0.04 Å) with Phe3, is strongly supported by the H–D exchange rates and VT NMR temperature coefficients (Table 1). There was a threefold slower H–D exchange of *t*BuGly2 NH and Ile5 NH in **4** than in **3**, and less temperature dependence of the chemical shift for the *t*BuGly2 amide NH. These data are consistent with stronger *t*BuGly2 NH···OC Ile5 and *t*BuGly2 CO···HN Ile5 hydrogen bonds in **4** than **3**. The re-introduced Phe3 NH had a similar H–D exchange rate to Phe3 in **2**. We conclude that a steric clash between *N*-Me of Phe3 and *t*Bu of *t*BuGly2, and a lower *t*BuGly2–Phe3 amide bond rotational energy, slightly altered the conformational ensemble in **3** and increased structural flexibility. However, no such clash occurs in **4** and so the *t*Bu better protects the two NH···OC pairs and creates a more contiguous hydrophobic patch than in **3**.

Finally, we investigated how structural changes in **2**–**4** affected membrane permeability, oral bioavailability, and pharmacokinetic parameters. The polarity readout EPSA (experimental polar surface area),[12] derived from supercritical fluid chromatography column retentions determined for **1** (77), **2** (74), **3** (64), and **4** (70), correlated with experimental RRCK[13] cell membrane permeabilities (*Papp* ($cm\,s^{-1}$): 0.6×10^{-6}, **1**; 0.7×10^{-6}, **2**; 9.6×10^{-6}, **3**; 1.2×10^{-6}, **4**) but neither correlated with rank order of oral bioavailability (Figure 6, Table 2), which is also influenced by factors like solubility, metabolic clearance, and protein binding. Cyclic peptides **3** and **4** were administered to male Wistar rats (10 $mg\,kg^{-1}$ p.o. versus 1 $mg\,kg^{-1}$ i.v.) under conditions we reported previously[7] for sanguinamide A (**2**). We found that predictions made about solvent exposure from NMR studies of amide H–D exchange (Table 1), of shielding of polar amides observed in NMR solution structures (Figure 3, Figure 4), and of hydrogen bond strengths based on measured distances in solution (e.g., Figure 5), correlated well with oral bioavailabilities of **3** and **4** (Figure 6). Compound **3** exhibited an improved pharmacokinetic profile compared to sanguinamide A (**2**) with about threefold improvements in oral bioavailability (F%) and half-life ($t_{1/2}$), ca. 25-fold increases in area under the curve (AUC_{0-8h}) and maximum plasma concentration (C_{max}), and a sixfold decrease in clearance from plasma (Table 2).

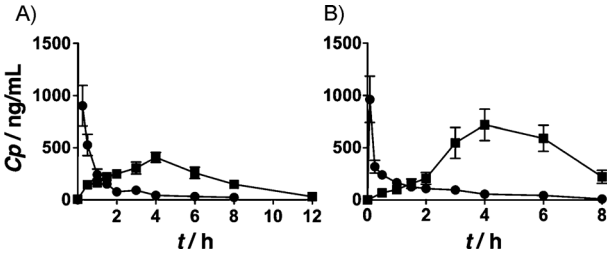

Figure 6. Plasma concentrations versus time for cyclic peptides **3** (A) and **4** (B) after oral administration of 10 $mg\,kg^{-1}$ in olive oil (squares) versus 1 $mg\,kg^{-1}$ i.v. in DMSO (circles) to male Wistar rats measured by LC-MS.

Table 2: Pharmacokinetic data for **2**–**4** and cyclosporin A given p.o. (10 $mg\,kg^{-1}$ in olive oil) versus i.v. (1 $mg\,kg^{-1}$ in DMSO) to male Wistar[a] rats.

Entry	$t_{1/2}$ [min]	CL [$mL\,min^{-1}\,kg^{-1}$]	C_{max} [$ng\,mL^{-1}$]	T_{max} [min]	AUC[b] [$ng\,h\,mL^{-1}$]	F%
2[c]	23	70.0	13.9	60	92	7 ± 4
3	65	12.5	352	240	2647	21 ± 2
4	97	23.0	726	240	3372	51 ± 9
CSA[d]	153	8.6	763	240	4095	21 ± 3

[a] For **2**, $n=4$ (p.o), $n=4$ (i.v.). For **3**, $n=6$ (p.o.), $n=4$ (i.v.). For **4**, $n=4$ (p.o.) $n=3$ (i.v.). [b] p.o. 10 $mg\,kg^{-1}$. [c] Ref. [7]. [d] Our data is shown. Reported elsewhere for CSA in rats at 10 $mg\,kg^{-1}$ i.v. versus 10 $mg\,kg^{-1}$ p.o., AUC 13 800 $ng\,h\,mL^{-1}$ (p.o.), F% 29;[14a] and at 6 $mg\,kg^{-1}$ i.v. versus 10 $mg\,kg^{-1}$ p. o., AUC 5500 $ng\,h\,mL^{-1}$ (p.o.), F% 23.[14b]

Surprisingly, removal of the *N*-Me in **3** to produce **4** more than doubled the oral bioavailability (F%), increasing the AUC, C_{max}, and $t_{1/2}$ values, but doubling the clearance (CL). Experimental Log*P* values for **1**–**4** were 1.7 (**1**), 2.5 (**2**), 3.2 (**3**), and 2.6 (**4**), suggesting **3** as the most hydrophobic/lipophilic, whereas **2** and **4** had similar LogP but quite different H–D exchange rates, C_{max}, AUC, and F% values. All compounds lie outside the traditional orally bioavailable small-molecule space: **1** (MW = 709, HBD = 5, "HBA" = 14, CLogP = 5.8, RotB = 6, tPSA = 186 Å^2), **2** (MW = 721, HBD = 4, "HBA" = 14, CLogP = 5.5, RotB = 6, tPSA = 169 Å^2), **3** (MW = 778, HBD = 3, "HBA" = 13, CLogP = 7.4, RotB = 7, tPSA = 161 Å^2), and **4** (MW = 764, HBD = 4, "HBA" = 13, CLogP = 6.8, RotB = 7, tPSA = 169 Å^2). Indeed, all have multiple violations of Lipinski[8a] and Veber[8b] parameters and provide new information on oral bioavailability limits for peptides.

In conclusion, we have transformed the cyclic heptapeptide **1**, which exists in multiple conformers, to a more rigid scaffold by introducing a heterocycle (thiazole), two intramolecular hydrogen bonds, and a compact branched (*tert*-butyl glycine) amino acid side chain that shields both H-bonds and polar atoms in **3** and **4**. These constraints led to greater oral absorption and bioavailability in rats. Rather than relying on traditional guidelines (rule-of-five, in silico calculations, membrane permeability) for improving the oral bioavailability, our improvements were based solely on NMR observa-

tions (amide H–D exchange rates, three-dimensional structures, solvent-exposed polar surfaces). The results demonstrate that NMR studies could be valuable for guiding the optimization of cyclic peptides for oral bioavailability, although they still need validation for biologically active compounds. This is the first report in which the oral bioavailability has been rationally optimized solely based on NMR spectroscopic observations of solvent-exposed surfaces.

Received: May 16, 2014
Revised: July 24, 2014
Published online: September 12, 2014

Keywords: cyclic peptides · NMR · oral bioavailability · permeability

[1] D. J. Craik, D. P. Fairlie, S. Liras, D. Price, *Chem. Biol. Drug Des.* **2013**, *81*, 136 – 147.
[2] a) J. D. A. Tyndall, T. Nall, D. P. Fairlie, *Chem. Rev.* **2005**, *105*, 973 – 1000; b) P. K. Madala, J. D. A. Tyndall, T. Nall, D. P. Fairlie, *Chem. Rev.* **2010**, *110*, PR1 – PR31.
[3] a) A. Ruegger, M. Kuhn, H. Lichti, H. R. Loosli, R. Huguenin, C. Quiquerez, A. V. Wartburg, *Helv. Chim. Acta* **1976**, *59*, 1075 – 1092; b) D. Faulds, K. L. Goa, P. Benfield, *Drugs* **1993**, *45*, 953 – 1040.
[4] A. Alex, D. S. Milan, M. Perez, F. Wakenhut, G. A. Whitlock, *Med. Chem. Commun.* **2011**, *2*, 669 – 674.
[5] a) T. R. White, C. M. Renzelman, A. C. Rand, T. Rezai, C. M. McEwen, V. M. Gelev, R. A. Turner, R. G. Linington, S. F. Leung, A. S. Kalgutkar, J. N. Bauman, Y. Zhang, S. Liras, D. A. Price, A. M. Mathiowetz, M. P. Jacobson, R. S. Lokey, *Nat. Chem. Biol.* **2011**, *7*, 810 – 817; b) E. Biron, J. Chatterjee, O. Ovadia, D. Langenegger, J. Brueggen, D. Hoyer, H. A. Schmid, R. Jelinek, C. Gilon, A. Hoffman, H. Kessler, *Angew. Chem. Int. Ed.* **2008**, *47*, 2595 – 2599; *Angew. Chem.* **2008**, *120*, 2633 – 2637.
[6] a) J. G. Beck, J. Chatterjee, B. Laufer, M. U. Kiran, A. O. Frank, S. Neubauer, O. Ovadia, S. Greenberg, C. Gilon, A. Hoffman, H. Kessler, *J. Am. Chem. Soc.* **2012**, *134*, 12125; b) T. Rezai, B. Yu, G. L. Millhauser, M. P. Jacobson, R. S. Lokey, *J. Am. Chem. Soc.* **2006**, *128*, 2510 – 2511.
[7] D. S. Nielsen, H. N. Hoang, R.-J. Lohman, F. Diness, D. P. Fairlie, *Org. Lett.* **2012**, *14*, 5720 – 5723.
[8] a) C. A. Lipinski, F. Lombardo, B. W. Dominy, P. J. Feeney, *Adv. Drug Delivery Rev.* **1997**, *23*, 3 – 25; b) D. F. Veber, S. R. Johnson, H. Y. Cheng, B. R. Smith, K. W. Ward, K. D. Kopple, *J. Med. Chem.* **2002**, *45*, 2615 – 2623.
[9] a) D. S. Wishart, B. D. Sykes, F. M. Richards, *Biochemistry* **1992**, *31*, 1647 – 1651; b) A. T. Brunger in X-PLOR Manual, v 3.1; Yale University Press, New Haven, **1992**; c) B. R. Brooks, R. E. Bruccoleri, B. D. Olafson, D. J. States, S. Swaminathan, M. J. Karplus, *Comput. Chem.* **1983**, *4*, 187 – 217.
[10] H. N. Hoang, R. W. Driver, R. L. Beyer, A. K. Malde, G. T. Le, G. Abbenante, A. E. Mark, D. P. Fairlie, *Angew. Chem. Int. Ed.* **2011**, *50*, 11107 – 11111; *Angew. Chem.* **2011**, *123*, 11303 – 11307.
[11] a) H. Morita, A. Shishido, T. Kayashita, K. Takeya, H. Itokawa, *J. Nat. Prod.* **1997**, *60*, 404 – 407; b) G. R. Pettit, et al., *J. Nat. Prod.* **1993**, *56*, 260 – 267; c) G. R. Pettit, J. P. Xu, Z. A. Cichacz, M. D. Williams, J. C. Chapuis, R. L. Cerny, *Bioorg. Med. Chem. Lett.* **1994**, *4*, 2677 – 2682; d) G. R. Pettit, R. Tan, Y. Ichihara, M. D. Williams, D. L. Doubek, L. P. Tackett, J. M. Schmidt, R. L. Cerny, M. R. Boyd, J. N. A. Hooper, *J. Nat. Prod.* **1995**, *58*, 961 – 965; e) H. J. Zhang, Y. H. Yi, G. J. Yang, M. Y. Hu, G. D. Cao, F. Yang, H. W. Lin, *J. Nat. Prod.* **2010**, *73*, 650 – 655; f) G. R. Pettit, J. K. Srirangam, D. L. Herald, J. P. Xu, M. R. Boyd, Z. Cichacz, Y. Kamano, J. M. Schmidt, K. L. Erickson, *J. Org. Chem.* **1995**, *60*, 8257 – 8261; g) R. Mohammed, J. N. Peng, M. Kelly, M. T. Hamann, *J. Nat. Prod.* **2006**, *69*, 1739 – 1744.
[12] G. H. Goetz, W. Farrell, M. Shalaeva, S. Sciabola, D. Anderson, J. Yan, L. Philippe, M. J. Shapiro, *J. Med. Chem.* **2014**, *57*, 2920 – 2929.
[13] L. Di, C. Whitney-Pickett, et al., *J. Pharm. Sci.* **2011**, *100*, 4974 – 4985.
[14] a) M. Jin, T. Shimada, M. Shintani, K. Yokogawa, M. Nomura, K. Miyamoto, *Drug Metab. Pharmacokinet.* **2005**, *20*, 324 – 330; b) S. Kalkan, M. Gumustekin, O. Aygoren, Y. Tuncok, A. Gelal, H. Guven, *Eur. J. Drug Metab. Pharmacokinet.* **2004**, *29*, 119 – 123.

